Liquid Crystals
Publication details, including instructions for authors and subscription information:
http://www.informaworld.com/smpp/title~content=t713926090

Side-chain liquid crystal polymers. A study by neutron diffraction of the backbone distribution profile in the smectic A phase

L. Noirez[a]; P. Davidson[b]; W. Schwarz[a]; G. Pépy[a]
[a] Laboratoire Léon Brillouin (CEA-CNRS), Cédex, France [b] Laboratoire Physique des Solides (associé au CNRS), Orsay Cédex, France

To cite this Article Noirez, L. , Davidson, P. , Schwarz, W. and Pépy, G.(1994) 'Side-chain liquid crystal polymers. A study by neutron diffraction of the backbone distribution profile in the smectic A phase', Liquid Crystals, 16: 6, 1081 — 1092
To link to this Article: DOI: 10.1080/02678299408027877
URL: http://dx.doi.org/10.1080/02678299408027877

LIQUID CRYSTALS, 1994, VOL. 16, NO. 6, 1081–1092

Side-chain liquid crystal polymers

A study by neutron diffraction of the backbone distribution profile in the smectic A phase

by L. NOIREZ*†, P. DAVIDSON‡, W. SCHWARZ† and G. PÉPY†

† Laboratoire Léon Brillouin (CEA-CNRS), CEN-Saclay, 91191 Gif-sur-Yvette, Cédex, France

‡ Laboratoire Physique des Solides (associé au CNRS), Bât. 510, Université Paris XI, 91405 Orsay Cédex, France

(*Received 29 July 1993: accepted 6 October 1993*)

Two mesomorphic side-chain polymethacrylates, called PMA(*R*)OC_4H_9, and only differing in the fact that one was deuteriated on the backbone ($R = D$) have been studied by neutron diffraction in the smectic A phase. The comparison between their respective smectic reflection intensities allows one to deduce quantitatively the backbone distribution profile along the normal to the layers. As the temperature decreases, the polymer backbones are more and more segregated from the sublayers of mesogenic cores. However, even at room temperature, there are still about 25 per cent of the backbone segments localized in the mesogenic core sublayers. These measurements, together with the previous determinations of the gyration radii of the backbones provide a detailed description of how the backbones of $PMAOC_4H_9$ are affected by the smectic ordering. In addition, the evolution with temperature of the different smectic reflection intensities is also discussed.

1. Introduction

The question of how the backbone of a mesomorphic side-chain polymer can accommodate the smectic ordering is at least 20 years old [1]. Two extreme situations were very early postulated [1]: the backbone may not be affected at all by the smectic field; then it keeps an almost spherical conformation and the backbone segments are located at random with respect to the layers (see figure 1 (*a*)). Conversely, the backbone may be squeezed between sublayers of mesogenic cores; then its configuration should be highly oblate and the backbone segment distribution should be strongly modulated by the smectic ordering (see figure 1 (*b*)).

On the one hand, the backbone conformation in the S_A phase has been widely studied during recent years [2–4] by small angle neutron scattering (SANS) on polymers deuteriated on the backbone. It was shown that the backbone conformation is always oblate, but that the anisotropy of the gyration radii $R_{\parallel}/R_{\perp}$ ($R_{\parallel}$ along the layer normal, $R_{\perp}$ perpendicular to it) of course depends on the chemical nature of the polymer.

On the other hand, the distribution of the backbone segments has been studied by X-ray diffraction for several polymers. Measurements of the smectic reflection intensities, followed by an inverse Fourier transform, give access to the electronic density profile along the normal to the layers [5–7]. It was thus shown that the polymer

* Author for correspondence.

0267–8292/94 $10·00

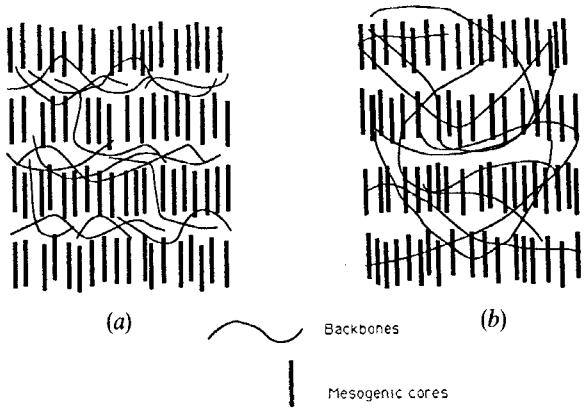

Figure 1. Schematic molecular organization of the polymeric S_A phase. (*a*) The backbones are confined between the sublayers of the mesogenic cores. (*b*) The backbones are not very much affected by the smectic order.

backbones were often confined in sublayers, but that the confinement degree varied with the chemical nature of the polymer. However, X-ray diffraction has two drawbacks: firstly, absolute measurements could not be made so that the profiles obtained only represented the variation of electronic density relative to the average value of the medium. Secondly, the electronic density does not directly reflect the backbone distribution. These two shortcomings can be avoided by use of neutron diffraction absolute measurements and by the isotopic labelling technique, as was first demonstrated by Ohm, Kirste and Oberthür [8]. Two polymers differing only by the fact that one has a deuteriated backbone, can be studied by neutron diffraction. Comparison of their smectic reflection intensities will give the backbone partial structure factor and, by inverse Fourier transform, the backbone density profile along the normal to the layers.

The present work differs from that of [8] by the nature of the polymer and, from a technical point of view, by the use of an appropriate neutron diffractometer and of oriented mono-domains instead of powders. These conditions provide more accurate measurements of the smectic reflection intensities. Moreover, the influence of temperature is also presented, and since the gyration radii of the backbone are already known, the backbone density profile will be discussed in relation to them.

2. Experimental conditions

The liquid crystalline polymethacrylate labelled $PMAOC_4H_9$ has been extensively studied for several years, by both X-ray diffraction, to determine the structures of its mesophases [7, 9] and by SANS, to measure the backbone dimensions [3, 4]. It presents the following well-described succession of mesophases:

G (glassy state)-35°C–S_A (smectic A)-100°C–N (nematic)-110°C–I (isotropic)

and corresponds to the chemical formula:

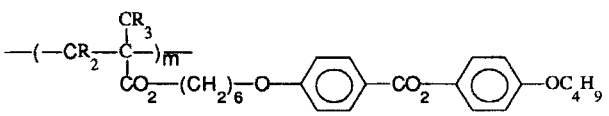

The polymer is called PMA(H)OC_4H_9 when $R=H$; it has a molecular weight of 257000 and a polydispersity of 2·2. When $R=D$, it is called PMA(D)OC_4H_9; its molecular weight is 355000 and its polydispersity 4·4.

These macromolecular characteristics have been determined using the technique of on line gel permeation chromatography/light scattering (in collaboration with C. Strazielle at the Institut Charles Sadron, Strasbourg).

It was previously checked [7] by X-ray diffraction that these two polymers are quite similar.

Two samples have been prepared, one made with the hydrogenous PMA(H)OC_4H_9 polymer, and the other with the polymer PMA(D)OC_4H_9 deuteriated on the backbone. These samples were placed in quartz disc-like cells of 17 mm diameter and 1 mm thickness. It can be assumed that the samples contain the same number of scatterers (the two samples having the same density and mass).

Each disc-like sample was mounted in an oven placed between the poles of an electromagnet (1·3 T). The magnet–oven set-up sits on the goniometer stage of a three-axis spectrometer (G-4·3 of the Laboratory Léon Brillouin) which was used in a two-axis configuration, i.e. recording the elastic scattering only. The incident wavelength was 4·15 Å. Two specific scanning directions were used: the first one, longitudinal, is parallel to the magnetic field (the director) and the second one, transverse, is perpendicular to it.

The sample is first heated up to the isotropic phase and then slowly cooled ($-0·2$°C to $-0·5$°C h^{-1}) down to the S_A phase in the magnetic field. During this 'step by step' temperature decrease, the intensities scattered in the regions of reciprocal space corresponding to the 001, 002 and 003 smectic reflections were measured following a longitudinal scan and a transverse scan carried out on each reflection. It has also been checked that higher reflection orders are of such weak intensity, if they exist, that they remain below the background noise.

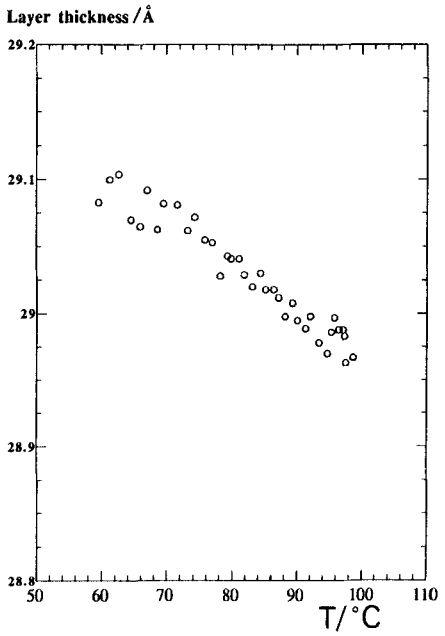

Figure 2. Variation of the smectic period with temperature for polymer PMAOC_4H_9.

3. Experimental results

As already reported [7,9], the values of the smectic period d shown in figure 2 correspond to the length of the polymer side chain, and therefore the S_A phase is of the monolayer type noted S_{A_1}. The layer spacing d increases very slightly (less than 0·2 Å from 98°C to 58°C) when the temperature decreases. The classical interpretation [10, 11] of this increase is a restriction of the motions, mostly of the terminal chain OC_4H_9.

Figures 3 and 4 present the intensity variation with temperature of the different smectic reflections for the hydrogenous polymer, $PMA(H)OC_4H_9$, and for the polymer deuteriated on the backbone, $PMA(D)OC_4H_9$, respectively. Note that, for the 001 reflection, the intensity scales of figures 3 and 4 differ by a factor 20 and that the 002 reflection of $PMA(D)OC_4H_9$ is not observed.

The intensity values are absolute values. They are obtained by normalizing the raw intensities by a ratio K, so that the measured intensity of the smectic reflections is proportional to the real intensity: $I_{meas} = K.I_{real}$. The background is modified in the same way, but also contains all the additional noise which does not come from the sample itself: $B_{meas} = K.B_{real} + C_{ste}$. In order to determine K, we use the fact that the two samples (hydrogenous and deuteriated) are examined under quite identical conditions. The difference in backgrounds is then due only to the isotopic difference between the two samples and can be compared to the difference in theoretical backgrounds.

This difference in theoretical backgrounds consists of the difference between the incoherent cross-section of the hydrogens of the hydrogenous polymer $d\sigma^H_{inc}/d\Omega$ and the incoherent cross-section of the deuteriums of the deuteriated polymer $d\sigma^D_{inc}/d\Omega$.

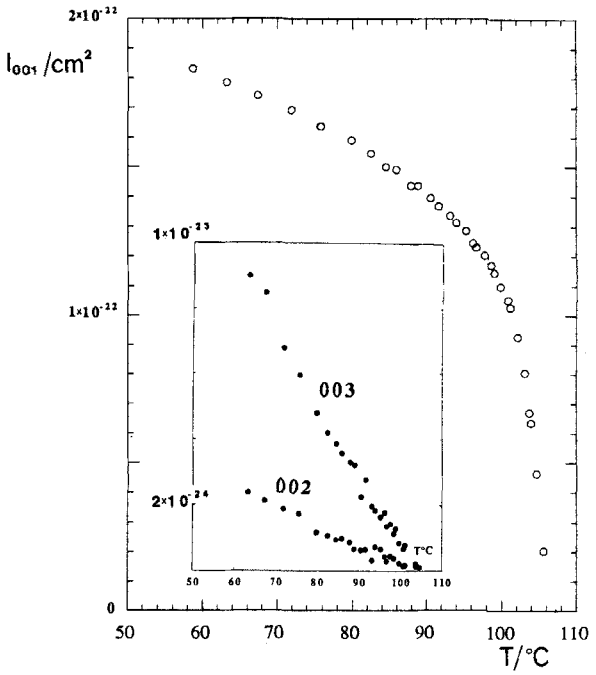

Figure 3. Variation of the normalized integrated intensities with temperature of the different orders of smectic reflections for the polymer $PMA(H)OC_4H_9$

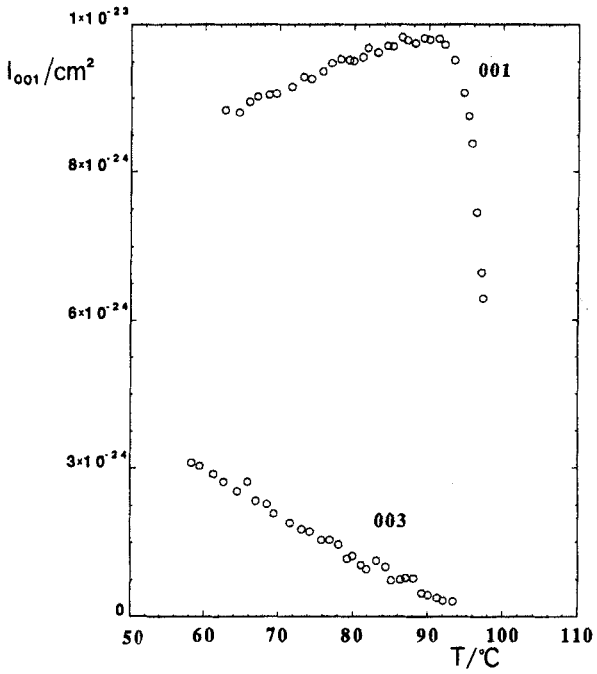

Figure 4. Variation of the normalized integrated intensities with temperature of the different orders of smectic reflections for the polymer PMA(D)OC_4H_9.

This value is compared to the experimental difference in backgrounds between the two samples $(I_0^H - I_0^D)$, in order to deduce the normalization factor

$$K = \frac{[(d\sigma_{inc}^H/d\Omega) - (d\sigma_{inc}^D/d\Omega)]}{(I_0^H - I_0^D)}.$$

This procedure allows one to ignore all supplementary background contributions like the experimental environment, the quartz window scattering, the detector electronic noise and so on.

The absolute values of the partial structure factors are calculated by taking the square root of the so-normalized intensities. Then division by the scattered volume of each sample gives to these structure factors the dimension of a specific density expressed in cm^{-2}. The combination of the partial structure factors gives the periodic profile of the coherent scattering length. This profile has the shape of a periodic wave oscillating around a zero mean value and therefore represents only a relative modulation. In order to obtain an absolute profile of coherent scattering length, the real mean value can be determined by the evaluation of the specific density of the coherent scattering length of each sample. This mean specific density is calculated by summing over the individual coherent scattering length of each atom of the sample. So, for the hydrogenous polymer, $\Psi_{OH} = N.(\Sigma bi_H/m_H).\rho = 1{\cdot}345 \times 10^{-10}\,cm^{-2}$, where ρ is the specific mass density ($g\,cm^{-3}$), m_H the monomer mass of the hydrogenous polymer and N the Avogadro number. By contrast, the specific density corresponding to the deuteriated polymer is $\Psi_{OD} = 2{\cdot}022 \times 10^{-10}\,cm^{-2}$.

4. Determination of the backbone density profiles

4.1. *Basic assumptions*

The determination of the density profiles of coherent scattering length along the director axis (z) is based on the following assumptions [5–8].

The S_A phase can be described as a continuous medium, periodically modulated along the z direction. The density $\Psi(z)$ (electronic density or coherent scattering length density, for example) can therefore be expressed as a Fourier series. Moreover, one can assume that there is no preferred orientation of the side chains (up or down) inside the layers, which implies that $\Psi(z)$ must be symmetrical. Then, only cosine terms enter the Fourier series

$$\Psi(z)=\Psi_0+\sum_i F_i \cos\left(\frac{2\pi}{d}.i.z\right).$$

Ψ_0 is the average density, d is the smectic period and the coefficients F_i are the structure factors which here must be real.

In reciprocal space, the Fourier transform of $\Psi(z)$ is a series of delta peaks

$$\sum_i F_i . \delta\left(q_z-\frac{2\pi}{d}.i\right)$$

and we actually measure Bragg peaks of order $00i$ and of intensity F_i^2.

Consequently, the experimental measurement of the integrated intensities of the $00i$ reflections provides $\pm F_i$, from which the different sign combinations supposed to represent $\Psi(z)$ are generated. In order to find which sign combination is physically acceptable, one must have an idea of what $\Psi(z)$ should look like. A simple molecular model (see figure 5) of the smectic layer, based on X-ray diffraction data [7], is used to evaluate roughly the respective densities of the side chains and backbones. This procedure implies that the different sign combinations give profiles sufficiently different to distinguish the good solution easily.

In addition, the difference between the structure factors of the hydrogenous polymer and those of the polymer deuteriated on the backbone constitute the partial

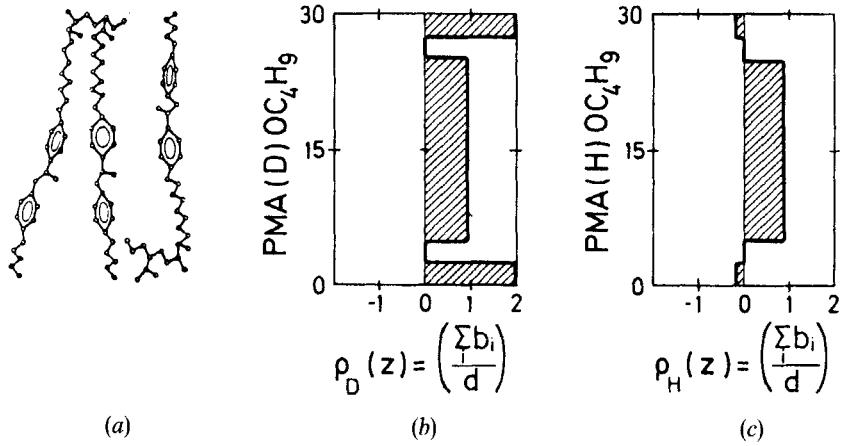

(*a*) (*b*) (*c*)

Figure 5. (*a*) Simple molecular model showing the liquid crystal polymer repeat unit in the smectic layers. (*b*) Corresponding schematic representation of the profile of coherent scattering length density for $PMA(D)OC_4H_9$. (*c*) Corresponding schematic representation of the profile of coherent scattering length density for $PMA(H)OC_4H_9$.

structure factors of the backbone. Then, their Fourier transform will directly provide the backbone density profile along the normal to the layers.

4.2. *Applications to PMA(H)OC_4H_9 and PMA(D)OC_4H_9*

We have determined the absolute modulation of coherent scattering length in the two following cases:

$\Psi_H(z)$ for the hydrogenous polymer PMA(H)OC_4H_9 (see figure 6),
$\Psi_D(z)$ for the deuteriated polymer PMA(D)OC_4H_9 (see figure 7), respectively, at high and low temperatures.

These two figures are calculated with the extreme values of the two intensity curves (see figures 3 and 4) from which a continuous evolution of the profile with temperature can be deduced.

The previous functions $\Psi_H(z)$ and $\Psi_D(z)$ represent the density of coherent scattering length associated respectively with PMA(H)OC_4H_9 and PMA(D)OC_4H_9. These functions can be decomposed into partial structure factors called f_i^{bb} for the backbone and F_i^{sc} for the side chain

for PMA(H)OC_4H_9:

$$\Psi_H(z)=\Psi_{OH}+\sum_i (F_{iH}^{bb}+F_{iH}^{sc})\cos\left(\frac{2\pi}{d}.i.z\right),$$

for PMA(D)OC_4H_9:

$$\Psi_D(z)=\Psi_{OD}+\sum_i (F_{iD}^{bb}+F_{iH}^{sc})\cos\left(\frac{2\pi}{d}.i.z\right),$$

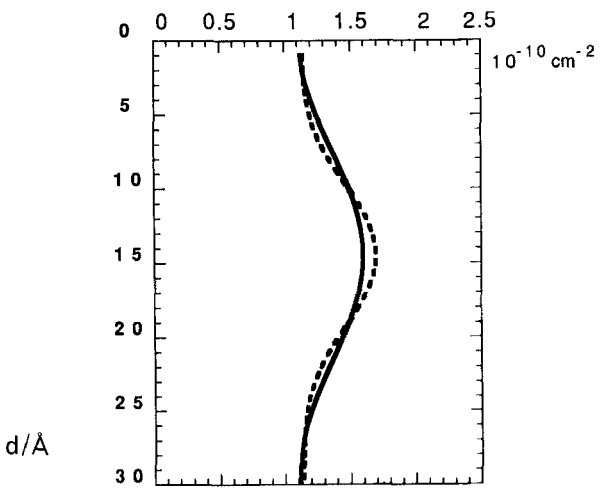

Figure 6. Absolute profile of coherent scattering length density for PMA(H)OC_4H_9 obtained 5 degrees below the N/S_A transition (solid line). At this temperature, the corresponding density is given by $\Psi_H(z)=(-0{\cdot}239\cos[(2\pi/d).z]+1{\cdot}354)$ $(10^{-10}\,cm^{-2})$, and at low temperature (dashed line) by $\Psi_H(z)=(-0{\cdot}276\cos[(2\pi/d).z]+0{\cdot}063\cos[(4\pi/d).z]+0{\cdot}035\cos[(6\pi/d).z]+1{\cdot}354)$ $(10^{-10}\,cm^{-2})$.

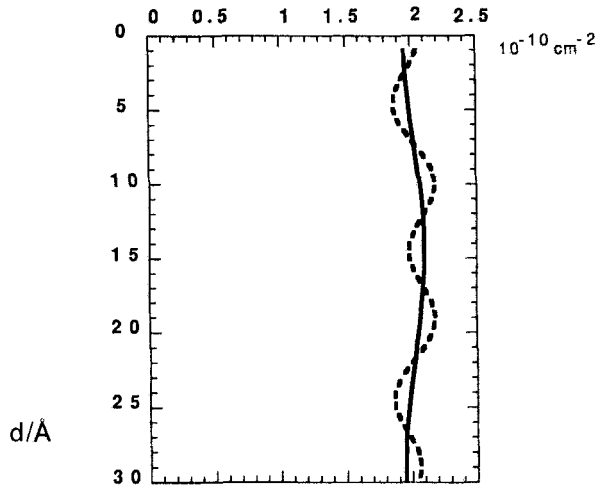

Figure 7. Absolute profile of coherent scattering length density for PMA(D)OC_4H_9 obtained 5 degrees below the N/S_A transition (solid line). At this temperature, the corresponding density is given by $\Psi_D(z) = (-0{\cdot}075\cos[(2\pi/d).z] + 2{\cdot}022)$ $(10^{-10}\,\mathrm{cm}^{-2})$, and at low temperature (dashed line) by $\Psi_D(z) = (-0{\cdot}075\cos[(2\pi/d).z] + 0{\cdot}120\cos[(6\pi/d).z] + 2{\cdot}022)$ $(10^{-10}\,\mathrm{cm}^{-2})$.

which can be more simply written

$$\Psi_H(z) = \Psi_{OH} + \Psi_H^{bb}(z) + \Psi_H^{sc}(z)$$

and

$$\Psi_D(z) = \Psi_{OD} + \Psi_D^{bb}(z) + \Psi_H^{sc}(z)$$

The difference $(\Psi_D(z) - \Psi_H(z))$ eliminates all the terms not belonging to the backbone and thus expresses the density of coherent scattering length (in cm^{-2}) corresponding to the backbones only

$$\Psi_D(z) - \Psi_H(z) = (\Psi_{OD} - \Psi_{OH}) + (\Psi_D^{bb}(z) - \Psi_H^{bb}(z))$$
$$= \Delta\Psi_O + \Delta\Psi(z)\ (\mathrm{cm}^{-2})$$

where $\Delta\Psi_O$, the difference between the hydrogenous and the deuteriated sample is: $\Delta\Psi_O = \Psi_{OD} - \Psi_{OH} = 0{\cdot}668 \times 10^{-10}\,\mathrm{cm}^{-2}$.

Therefore, we have (see figure 8)

at high temperature:

$$\Psi_D(z) - \Psi_H(z) = \left(0{\cdot}164\cos\left(\frac{2\pi}{d}.z\right) + 0{\cdot}668\right)(10^{-10}\,\mathrm{cm}^{-2});$$

and at low temperature:

$$\Psi_D(z) - \Psi_H(z) = \left(0{\cdot}201\cos\left(\frac{2\pi}{d}.z\right) - 0{\cdot}063\cos\left(\frac{4\pi}{d}.z\right) + 0{\cdot}086\cos\left(\frac{6\pi}{d}.z\right) + 0{\cdot}668\right)(10^{-10}\,\mathrm{cm}^{-2}).$$

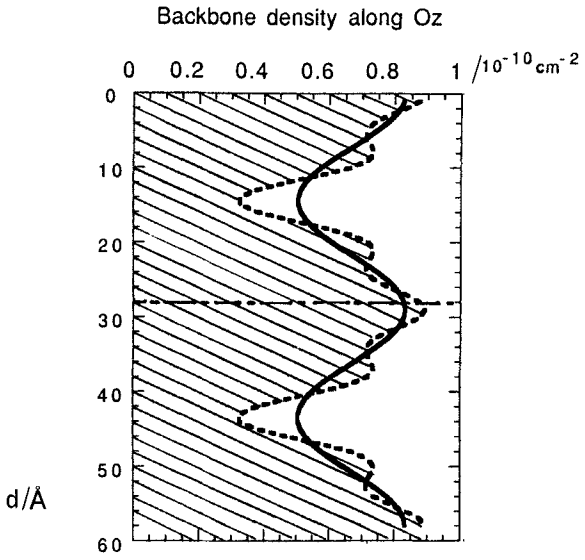

Figure 8. Absolute profiles of density of backbone scatterers along the normal to the layers at high temperature (solid line) and at low temperature (dashed line).

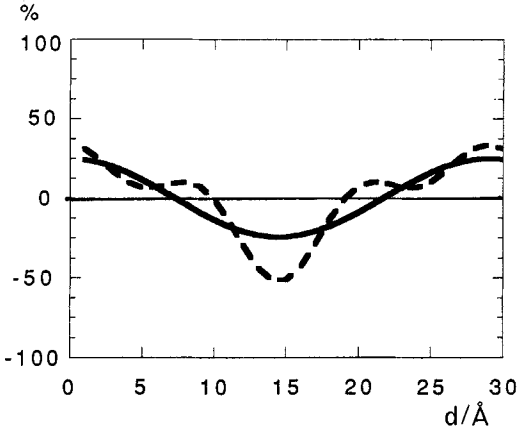

Figure 9. Percentage of backbone scatterers, in addition or in loss compared to the average value at high temperature (solid line) and at low temperature (dashed line).

The 'rate' of backbone scatterers, in addition or in loss, compared to the medium of average $\Delta\Psi_0$ is

$$\tau(z)=\left(\frac{\Delta\Psi(z)}{\Delta\Psi_0}-1\right).$$

$\tau(z)$ is represented in figure 9 and corresponds at high temperature to $\tau(z)=0{\cdot}247\cos[(2\pi/d).z]$ and at low temperature to

$$\tau(z)=\left(0{\cdot}302\cos\left(\frac{2\pi}{d}.z\right)-0{\cdot}095\cos\left(\frac{4\pi}{d}.z\right)+0{\cdot}128\cos\left(\frac{6\pi}{d}.z\right)\right).$$

5. Discussion

Figure 8 shows the backbone density profiles at high temperature (T_{NA}) and at room temperature. In between, there is a progressive evolution of the profile. At high temperature (solid line), the profile is described by a single sine wave. Since the sine wave is the simplest periodic modulation, one can consider that the backbones, though not uniformaly located, are not very much disturbed by the smectic order. In contrast, at low temperature (dashed line), the backbone profile is more complicated and shows clearly the segregation of the backbones from the sublayer of mesogenic cores. However, note that, even at low temperature, this segregation is not complete, since the backbone density does not reach zero in that region, as observed in [8]. The fraction of backbone units still located inside the mesogenic core sublayer is estimated to be about 25 per cent, which is a fair amount. At this point, the influence of layer undulations should be taken into account. Indeed, such transverse fluctuations should spread the backbone sublayer along the normal to the layers. However, these fluctuations have already been studied for this polymer [7] and their amplitude was evaluated as about 5 Å. This value can in part explain the width of the backbone sublayer (see figure 8), but not the presence of backbone segments in the central part of the layer. Therefore, this discussion implies that crossing of the backbones through the layers seems still possible. However, it should be remembered that the density profiles discussed here do not represent the mean behaviour of a single backbone. These profiles correspond instead to a scale of density of backbone units irrespective of their belonging to any given backbone. In other words, in contrast with SANS experiments, the experiment described here does not allow one to follow the trajectory of a single backbone. The phenomenon of layer crossing by the backbones has already been predicted theoretically [12] and suggested experimentally by the observation of a peculiar X-ray diffuse scattering [7].

From another point of view, the differences in thermal behaviour of the 00*i* smectic reflections are surprising. First, let us discuss the difference between the two 001 reflections of PMA(H)OC_4H_9 and PMA(D)OC_4H_9. The curve associated with the 001 reflection of PMA(D)OC_4H_9 presents an unusual behaviour since, at low temperature, its intensity decreases when the temperature decreases. This behaviour has already been reported for similar polymers [13–16] and interpreted by the slow annealing of defects. This was supposed to be brought about by the influence of the main chain characteristics on the mechanical properties (rigidity, viscosity...) of the phase. Such an effect is not observed in the case of PMA(H)OC_4H_9. Subsequent X-ray diffraction experiments on PMA(H)OC_4H_9 and PMA(D)OC_4H_9 showed that this phenomenon is not essentially related to the deuteriation, but more likely to the sample preparation or details of thermal history. Nevertheless, this effect is small and hardly affects the backbone density profile.

It is also interesting to notice that the rather sharp evolution of the 001 reflection more or less follows the evolution of the dimensions $R_{\parallel}$ and $R_{\perp}$ of the PMAOC_4H_9 backbone (see figure 10) versus temperature. An analogy was previously made between the behaviour of $\mathbf{R}_{\parallel}$ versus temperature and that of the 001 reflection intensity in the case of the mixture PMA(D)OC_4H_9/PMA(H)OC_4H_9 [17]. In contrast, the intensities of the 002 and 003 peaks increase linearly when the temperature decreases (over a 40 degrees range) until T_g is reached. If we consider that the 001 reflection corresponds to the layer size, the 002 and 003 reflections will correspond to modulations of period $d/2$ and $d/3$ related to the internal organization inside the smectic layer. Whereas the smectic modulation appears quite sharply, the 'softer' evolution of the 002 and the 003

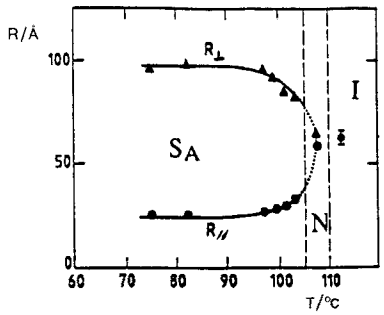

Figure 10. Evolution of the average gyration radii ($R_{\parallel}$ and $R_{\perp}$) of the polymer backbone with temperature for the mixture (1 : 1) of PMA(D)OC_4H_9: PMA(H)OC_4H_9.

reflections suggests that the internal arrangement inside the layer settles only progressively. Indeed, when the intensity of the 001 reflection saturates, the higher orders of reflection still increase linearly. This shows that rearrangements of the mesogenic core sublayer are still possible and do not alter the average gyration radii $R_{\parallel}$ and $R_{\perp}$. In this respect, these quantities do not seem so sensitive to the internal structure of the smectic layer, but rather to the existence of layer crossings by the backbones.

Finally, let us turn back to the thermal evolutions of the smectic reflections of polymer PMA(H)OC_4H_9 (see figure 3). From a theoretical point of view, the evolution of the 001 reflection intensity could be reminiscent of an order parameter behaviour and could suggest a second order transition. In such a case, a simple model [18] will show that if the 001 reflection intensity follows a power law with an exponent α (mean field model: $\alpha = 1$), then the $00n$ reflection intensity should follow a power law with an exponent $n\alpha$. Clearly, this is not experimentally observed here, so that the N/S_A transition is not well described by a simple model of a second order transition. From another point of view, the thermal evolutions of the reflection intensities may also be discussed in Debye–Waller terms. This term will affect these intensities in the following way [7]: $I_{00n} \approx \exp -(n^2/B.d^2)$ (B is the elastic constant for compression of the layers) which depends on the reflection order n. However, this expression too clearly cannot account for the apparent linear dependance of the 002 and 003 reflection intensities with temperature. Actually, the existence of a biphasic region around the transition and the large influence of defects and thermal history strongly prevent a proper description from being made.

6. Conclusions

The backbone segment density along the normal to the layers of polymer $PMAOC_4H_9$ in its S_A phase is not uniform, since the intensities scattered by the hydrogenous polymer and the polymer deuteriated in the backbone obviously differ. The evolution with temperature shows that the smectic ordering is accompanied by a segregation of the backbones away from the mesogenic core sublayers. The 'smooth' smectic order at high temperature corresponds to a smooth periodic distribution of the backbones (a sine wave profile). On decreasing temperature, the backbone density profile becomes more complicated, thus indicating that the backbones are more and more segregated from the mesogenic core sublayer. However, even at room temperature, the fraction of backbone segments located in the middle of the layer is still about 25 per cent, which probably means that the backbones still have the ability to cross the layers.

The different orders of smectic reflections present different behaviours with temperature. The behaviour of the first order is somewhat similar to that of the radius of gyration $R_{\parallel}$ [17], i.e. a fast evolution over a 10 degree range below the N/S_A transition and then saturation. In contrast, the second and third orders increase linearly when the temperature decreases until T_g is reached. This increase in the 002 and 003 orders has no effect on the global dimensions of the chain (radii of gyration $R_{\parallel}$ and $R_{\perp}$) and is apparently only due to an internal structural modification of the smectic layer.

Finally, it should be recalled that many of the results and interpretations presented in this work probably depend on the spacer length. This parameter, known to be of great importance for this class of compounds [19], should be systematically varied to check to what extent the present conclusions can be generalized.

The authors would like to thank P. Keller for kindly providing us with the hydrogenous and the deuteriated polymers, D. Petermann for technical help with the X-ray experiments and G. Durand, A. M. Levelut and T. Lubensky for helpful discussions.

References

[1] STRZELECKI, L., and LIÉBERT, L., 1973, *Bull. Soc. chim. Fr.*, **2,** 597, and references therein.
[2] KIRSTE, R. G., and OHM, H. G., 1985, *Makromolek. Chem. rap. Commun.*, **6,** 179.
[3] KELLER, P., CARVALHO, B., COTTON, J. P., LAMBERT, M., and PÉPY, G., 1985, *J. Phys. Lett., France*, **46,** 1065.
[4] NOIREZ, L., MOUSSA, F., COTTON, J. P., KELLER, P., and PÉPY, G., 1991, *J. statist. Phys.*, **62,** 997.
[5] GUDKOV, V. A., 1984, *Soviet Phys. Crystallogr.*, **29,** 316.
[6] TSUKRUK, V. V., and SHILOV, V. V., 1990, *Polymer*, **31,** 1793.
[7] DAVIDSON, P., and LEVELUT, A. M., 1992, *Liq. Crystals*, **11,** 469.
[8] OHM, H. G., KIRSTE, R. G., and OBERTHÜR, R. C., 1988, *Makromolek. Chem.*, **116,** 1387.
[9] ZENTEL, R., and STROBL, G. R., 1984, *Makromol. Chem.*, **185,** 2669.
[10] GUILLON, D., and SKOULIOS, A., 1977, *J. Phys., Paris*, **38,** 79.
[11] OULYADI, H., LAUPRETRE, F., MONNERIE, L., MAUZAC, M., RICHARD, H., and GASPAROUX, H., 1990, *Macromolecules*, **23,** 1965.
[12] RENZ, W., WARNER, M., 1986, *Phys. Rev. Lett.*, **56,** 1268.
[13] SHILOV, V. V., TSUKRUK, V. V., and LIPATOV, YU. S., 1984, *J. Polym. Sci.*, **22,** 41.
[14] RICHARDSON, R. M., and HERRING, N. J., 1985, *Molec. Crystals liq. Crystals*, **123.** 143.
[15] SUTHERLAND, H. H., and RAWAS, A., 1986, *Molec. Crystals liq. Crystals*, **138,** 179.
[16] ZUGENMAIER, P., and MENZEL, H., 1988, *Makromolek. Chem.*, **189,** 2647.
[17] NOIREZ, L., PÉPY, G., KELLER, P., and BENGUIGUI, L., 1991, *J. Phys., Paris, II*, **1,** 821.
[18] See, for example, the similar discussion of incommensurate crystals by AXE, J. D., IIZUMI, M., and SHIRANE, G., 1986, *Modern Problems in Condensed Matter Sciences*, Vol. 14–2 (Elsevier), p. 36.
[19] MITCHELL, G. R., COULTER, M., DAVIS, F. J., and GUO, W., 1992, *J. Phys., Paris, II*, **2,** 1121.